ANALYTICAL APPROACH TO INTENSITY CALCULATION IN SCINTILLATION DETECTORS

Vovchenko Ivan[1,2],
[1]Moscow Institute of Physics and Technology
(National Research University) Dolgoprudnyi, Moscow region, 141700 Russia,
[2]Institute of Theoretical and Applied Electrodynamics, Moscow, 125412 Russia
vovchenko@phystech.edu

Khamitov Timur[1,3],
[1]Moscow Institute of Physics and Technology
(National Research University) Dolgoprudnyi, Moscow region, 141700 Russia,
[3]Institute for Nuclear Research (INR) of the Russian Academy of Sciences,
Moscow, 117312, Russia,
hamitov.tm@phystech.edu

ABSTRACT

Scintillation detectors are widely used in modern physics, including various medical tomographs. There are two types of position-sensitive scintillation detectors: pixel arrays of "scintillator-photomultiplier" pairs and continuous scintillator with multiple photomultipliers attached. For the last one, there are two common ways to calculate the coordinates of the scintillation flash via detector response in scintillation cameras: Anger's method and Monte-Carlo simulation. In this article, we develop an analytical approach (so-called "kaleidoscopic ray-tracing") to compute the energy outcome from several light detectors in the scintillation camera with a continuous scintillator, which has reflective and absorbing faces. We show that Anger's method is just an approximation of the exact solution. Anger's method requires absorbing faces only, so our approach covers a more general case. The derived method achieves results, that are similar to the Monte-Carlo simulation, but it requires fewer computations.

Keywords Scintillation detector · Coordinate reconstruction · Gamma camera · SPECT · PET

1 Introduction

Contemporary computed tomography (CT scanning) engages two basic types of scintillation detectors: continuous scintillator with photomultipliers attached and pixel arrays. Pixel arrays can achieve better resolution and do not require any coordinate reconstruction methods, while detector with continuous scintillator does. Optimization and development of mentioned methods could reduce the costs of tomographs. Also, these two types of detectors can be combined [1].

Algorithms for coordinate reconstruction are easier to implement when the scintillator is black painted. However, it reduces the energy resolution. The development of an algorithm capable of restoring the coordinate of a scintillation flash in a detector with a solid scintillator with semi-reflecting walls can lead to an increase in the energy resolution of such detectors while maintaining the same coordinate resolution.

The problem of the coordinate reconstruction can be formalized next way. If a uniform flash with intensity I happens at the point (x_0, y_0, z_0), there is a mapping $\vec{F}(x_0, y_0, z_0, I)$ that translates x_0, y_0, z_0, I into a set of intensities each of detectors got $\vec{W} = \vec{F}(x_0, y_0, z_0, I)$. The inverse problem must be solved: an inverse mapping $\{x_0, y_0, z_0, I\} = \vec{F}^{-1}(\vec{W})$ must be found. In practice, it is done by minimising deviation under the norm

$$\|\vec{F}(\vec{F}^{-1}(\vec{W})) - \vec{W}\|. \tag{1}$$

To push the algorithms for coordinate reconstruction further, we should precisely solve the forward model first.

Detectors with continuous scintillators are usually designed as rectangular cuboid scintillators with various reflectivities for each face. The bottom face of the cuboid is divided into several detectors. A common problem of CT scanning is to localize the flash induced by gamma quantum inside the scintillator using intensities on detectors. It is solved in several ways usually. The ordinary approach is to use Anger's method [2–4]. For this method to be implemented, all faces should be fully absorbing and the number of detectors embedded in the bottom face of the scintillator should be large. The coordinates of the flash are calculated as "center of mass," where the energy on each detector is considered as "mass." A more complex approach involves Monte-Carlo modeling [5, 6]. First, an array of intensities for all possible points, where flash can happen, is modeled. Second, an inverse problem is solved. Inverse algorithms minimize the difference between intensity achieved in the experiment and a set of intensities from the modeled array under some norm.

In this article, we develop an analytical approach to the calculation of intensities on detectors embedded in the scintillator bottom face (i.e. mapping $\vec{F}(x_0, y_0, z_0, I)$). Further, we call this approach kaleidoscopic ray-tracing. It is based on kaleidoscopic reflection of the bottom face of the scintillator over semi-reflecting walls. Numerically, this approach consists in the calculation of several infinite sums. We show that the results, achieved via the developed approach are in agreement with the Monte-Carlo simulation, being achieved with less computing efforts. Numerical implementation of the method involves errors, that are also estimated analytically. Moreover, we showed that Anger's method (without clustering modification) shifts the flash by the distance, which is comparable with the size of an individual detector even under quite favorable conditions for Anger's method to be implemented. However, minimization of (1) requires an initial guess on parameters. The coordinates can be estimated using the Anger method to start the optimization process, I can be calculated as the result of the total energy, summed over all detectors and multiplied by some calibration factor.

2 Kaleidoscopic ray-tracing

We consider the rectangular cuboid box with semi-reflecting faces (including bottom and top). The box is placed as it is shown in Fig. 1. The bottom of the box is centered at $(0, 0, 0)$ point and has $z = 0$, the top has $z = H$. The bottom of the box is split into $n \times m$ (for simplicity and clarity all the figures display the case $n = 3$, $m = 2$) photodetectors with the size $a \times b$. Then, the length of the box is $L_x = na$ and the width is $L_y = nb$. The faces have corresponding reflective indexes p_{xL} (the wall that is perpendicular to the x-axis and has $x < 0$), p_{xR} (the wall that is perpendicular to the x-axis and has $x > 0$), p_{yL}, p_{yR}, p_{zL} (bottom face of the box), p_{zR} (top face of the box).

A flash with intensity I that is uniformly distributed over the spherical angle occurs at (x_0, y_0, z_0). To calculate the intensity each of the detectors gets, we kaleidoscopically reflect the bottom of the box over the walls as it is shown in Fig. 2. Green lines denote reflections of the entire bottom face over the walls, blue lines depict reflections of the detectors. Over this plane, all rays would be straightened. Now to compute the intensity on the detector, we should sum the intensities on all reflections of this detector, multiplying them by reflective indexes of the walls corresponding number of times, see Fig 3.

The detectors are indexed with i, j, reflections of the box are indexed with α, β. For instance: real box has $\alpha = 0$, $\beta = 0$, its reflection once over the wall with $x < 0$ and twice over the wall with $y < 0$ has $\alpha = -1$, $\beta = -2$, the reflection of the real box once over the wall $y > 0$ has $\alpha = 0$, $\beta = 1$.

2.1 Fully absorbing bottom face

A fully absorbing bottom face should be considered first. Following the above, the intensity on the i, j detector should be calculated as

$$I_{ij} = \sum_{\alpha=-\infty}^{+\infty} \sum_{\beta=-\infty}^{+\infty} p_{xL}^{n_{xL}} p_{xR}^{n_{xR}} p_{yL}^{n_{yL}} p_{yR}^{n_{yR}} \left(\Delta I_{\alpha\beta,ij}^{(x_0,y_0,z_0)} + p_{zR} \Delta I_{\alpha\beta,ij}^{(x_0,y_0,2H-z_0)} \right). \tag{2}$$

Here $\Delta I_{\alpha\beta,ij}^{(x_0,y_0,z_0)}$ is the amount of energy absorbed by $\alpha\beta$ reflection of ij detector from the flash that occurs at (x_0, y_0, z_0), if there is no top face. Since there is top face and it is semi-reflecting, one should take $\Delta I_{\alpha\beta,ij}^{(x_0,y_0,2H-z_0)}$ (the image source) under consideration. Its intensity should be multiplied by p_{zR} – the reflective index of the top face. Degrees n_{xL}, n_{xR}, n_{yL}, n_{yR} are numbers of times the horizontal projection of a ray intersect green lines in Fig. 2 with the corresponding reflective index before it reaches the $\alpha\beta$ reflection of ij detector. These numbers do not depend on the chosen ray, because the rays, that are absorbed by $\alpha\beta$ reflection of ij detector, being straightened by kaleidoscopic reflection, intersect same green lines same amount of times.

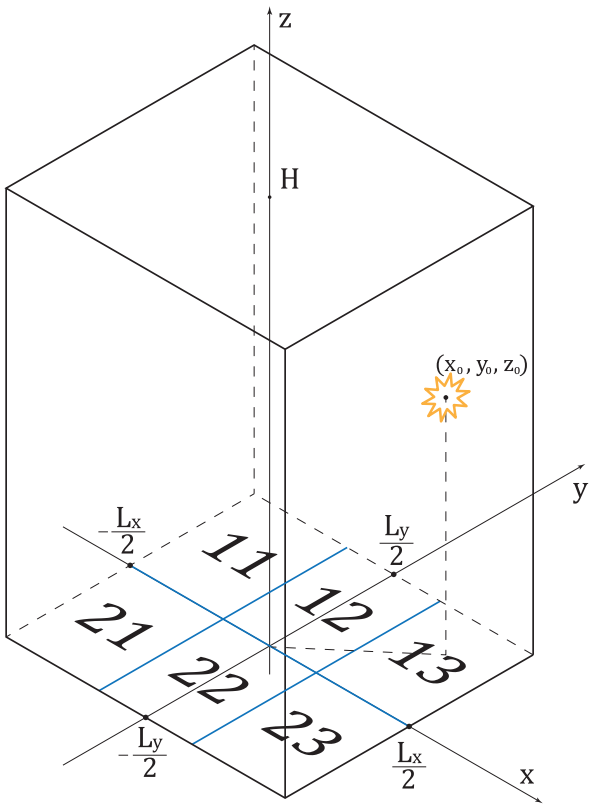

Figure 1: The box with semi-reflective faces, $n = 3$, $m = 2$. The flash occurs at (x_0, y_0, z_0) (yellow source). Detectors are indexed as elements of a matrix.

To calculate the amount of energy per arbitrary rectangle area with length a and width b (further this rectangle area is denoted as A), one should calculate the integral of the Umov-Pointing vector component that is normal to the rectangle area A [7, 8]. To do that, the source with intensity I at $\vec{r_0} = (x_0, y_0, z_0)$ is considered; rectangle A lies in the xy-plane and its sides are parallel to x and y-axis and its bottom left corner has $(x^{(L)}, y^{(L)})$ coordinates. The mentioned integral can be written as:

$$I_A = \int\limits_A (\vec{S}, \vec{n}_A) dx dy = \int\limits_{x^{(L)}}^{x^{(L)}+a} dx \int\limits_{y^{(L)}}^{y^{(L)}+b} dy \frac{I}{4\pi R^2} \frac{z_0}{R}. \tag{3}$$

Here $\vec{n}_A$ is a normal vector of the rectangle area A, $\vec{R} = \vec{r} - \vec{r_0}$, $R = \sqrt{(x-x_0)^2 + (y-y_0)^2 + z_0^2)}$, $\vec{S} = \frac{\vec{R}}{R} \frac{I}{4\pi R^2}$ - Umov-Pointing vector. The integral over y might be computed first:

$$\int\limits_{y^{(L)}}^{y^{(L)}+b} \frac{dy}{((x-x_0)^2 + (y-y_0)^2 + z_0^2))^{3/2}} = \begin{bmatrix} u = x - x_0 \\ v = y - y_0 \end{bmatrix} =$$

$$= \int\limits_{y^{(L)}-y_0}^{y^{(L)}-y_0+b} \frac{dv}{(u^2 + v^2 + z_0^2))^{3/2}} = \frac{v}{(u^2 + z_0^2)\sqrt{u^2 + v^2 + z_0^2}} \Bigg|_{y^{(L)}-y_0}^{y^{(L)}-y_0+b} =$$

$$= \frac{y^{(L)} - y_0 + b}{(u^2 + z_0^2)\sqrt{u^2 + (y^{(L)} - y_0 + b)^2 + z_0^2}} - \frac{y^{(L)} - y_0}{(u^2 + z_0^2)\sqrt{u^2 + (y^{(L)} - y_0)^2 + z_0^2}}. \tag{4}$$

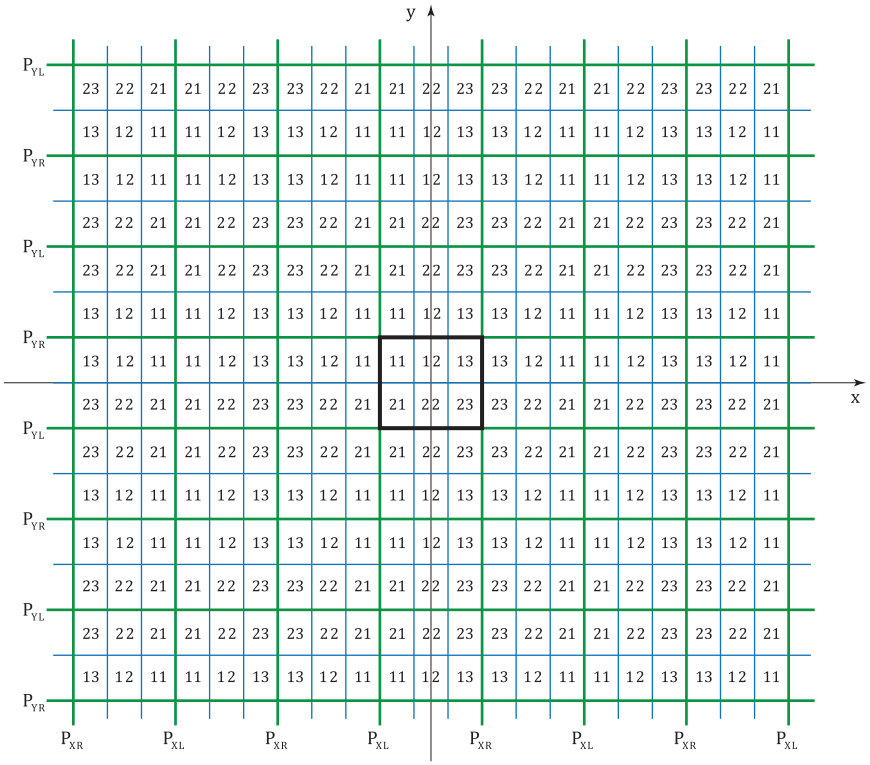

Figure 2: Kaleidoscopic reflection of the scintillator bottom face over the faces of the walls. Faces are marked with corresponding reflective indexes $p_{xL}, p_{xR}, p_{yL}, p_{yR}$.

Now the integral over u should be computed. Here c and p denote constants from Eq. (4):

$$\int\limits_{x^{(L)}-x_0}^{x^{(L)}-x_0+a} \frac{du}{(u^2+c)\sqrt{u^2+p}} = \left.\frac{\tan^{-1}\left(\frac{u\sqrt{p-c}}{\sqrt{c}\sqrt{p+u^2}}\right)}{\sqrt{c}\sqrt{p-c}}\right|_{x^{(L)}-x_0}^{x^{(L)}-x_0+a}. \tag{5}$$

Finally, the integral from Eq. (3) equals

$$\begin{aligned} I_A = \frac{\mathrm{sign}(y^{(L)}-y_0+b)}{z_0}\Bigg[\tan^{-1}\left(\frac{(x^{(L)}-x_0+a)|y^{(L)}-y_0+b|}{z_0\sqrt{(x^{(L)}-x_0+a)^2+(y^{(L)}-y_0+b)^2+z_0^2}}\right) - \\ - \tan^{-1}\left(\frac{(x^{(L)}-x_0)|y^{(L)}-y_0+b|}{z_0\sqrt{(x^{(L)}-x_0)^2+(y^{(L)}-y_0+b)^2+z_0^2}}\right)\Bigg] - \\ - \frac{\mathrm{sign}(y^{(L)}-y_0)}{z_0}\Bigg[\tan^{-1}\left(\frac{(x^{(L)}-x_0+a)|y^{(L)}-y_0|}{z_0\sqrt{(x^{(L)}-x_0+a)^2+(y^{(L)}-y_0)^2+z_0^2}}\right) - \\ - \tan^{-1}\left(\frac{(x^{(L)}-x_0)|y^{(L)}-y_0|}{z_0\sqrt{(x^{(L)}-x_0)^2+(y^{(L)}-y_0)^2+z_0^2}}\right)\Bigg]. \end{aligned} \tag{6}$$

The degrees of reflective indexes can be calculated next way:

$$n_{xL} = \left\lfloor \frac{|\alpha| + \frac{1-\mathrm{sign}(\alpha)}{2}}{2} \right\rfloor, \qquad n_{xR} = \left\lfloor \frac{|\alpha| + \frac{1+\mathrm{sign}(\alpha)}{2}}{2} \right\rfloor, \tag{7}$$

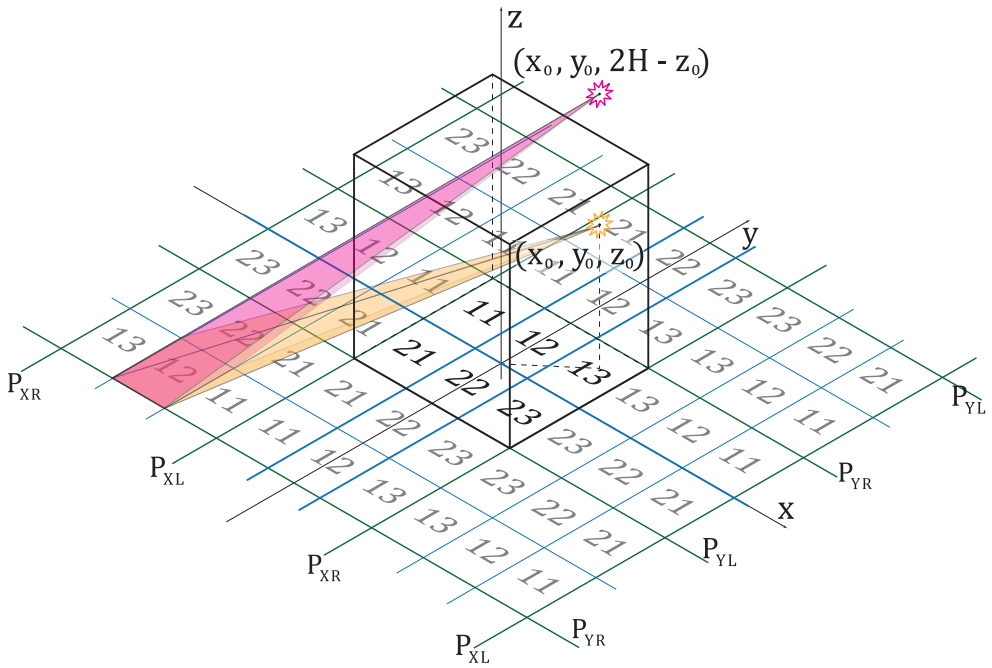

Figure 3: Kaleidoscopic reflection of the scintillator bottom face over the wall faces and spherical angle of the $\alpha = -1, \beta = -1$ reflection of the $i = 1, j = 2$ detector due to the flash (yellow source) and its reflection over the top face (pink source). Wall faces are marked with corresponding reflective indexes $p_{xL}, p_{xR}, p_{yL}, p_{yR}$ in xy-plane.

$$n_{yL} = \left\lfloor \frac{|\beta| + \frac{1-\mathrm{sign}(\beta)}{2}}{2} \right\rfloor, \qquad n_{yR} = \left\lfloor \frac{|\beta| + \frac{1+\mathrm{sign}(\beta)}{2}}{2} \right\rfloor. \tag{8}$$

Here $\lfloor Q \rfloor$ denotes the integer part of Q. Eq. (6) and Eqs. (7)-(8) give explicit answer being substituted in Eq. (2). One should only define $x^{(L)}$ and $y^{(L)}$ for each of reflections each of detectors. We start with defining centers of detectors $x^{(c)}_{00,ij}$ $y^{(c)}_{00,ij}$ as coordinates of points where diagonals of a detector intersect each other. Now one can establish coordinates of centers of detector reflections:

$$x^{(c)}_{\alpha\beta,ij} = x^{(c)}_{00,ij} \cdot (-1)^{|\alpha| \bmod 2} + \alpha L_x, \qquad y^{(c)}_{\alpha\beta,ij} = y^{(c)}_{00,ij} \cdot (-1)^{|\beta| \bmod 2} + \beta L_y, \tag{9}$$

$$x^{(L)}_{\alpha\beta,ij} = x^{(c)}_{\alpha\beta,ij} - a/2, \qquad y^{(L)}_{\alpha\beta,ij} = y^{(c)}_{\alpha\beta,ij} - b/2. \tag{10}$$

Here $x^{(L)}_{\alpha\beta,ij}$ and $y^{(L)}_{\alpha\beta,ij}$ are coordinates of bottom left corner of the $\alpha\beta$ reflection of the ij detector.

It should be mentioned that Eqs. (7)-(10) are not a consequence of any physical low and could be exchanged with other ones. However, we find the form mentioned above the most suitable one.

2.2 Case of the reflecting bottom face

If the bottom face has a nonzero reflective index Eq. (2) should be modified. One should replicate kaleidoscopic surface from Fig. 3 at heights $-2H$, $-4H$, $-6H$, ... This trick straightens the rays that are reflected from the bottom face, and the previously made procedure can be done now. Finally, we get:

$$I_{ij} = \sum_{n_{zL}=0}^{+\infty} (1 - p_{zL}) p_{zL}^{n_{zL}} p_{zR}^{n_{zL}} \sum_{\alpha=-\infty}^{+\infty} \sum_{\beta=-\infty}^{+\infty} p_{xL}^{n_{xL}} p_{xR}^{n_{xR}} p_{yL}^{n_{yL}} p_{yR}^{n_{yR}} \left(\Delta I^{(x_0,y_0,z_0)}_{\alpha\beta,ij} + p_{zR} \Delta I^{(x_0,y_0,2H-z_0)}_{\alpha\beta,ij} \right). \tag{11}$$

Here $\Delta I^{(x_0,y_0,z_0)}_{\alpha\beta,ij,n_{zL}}$ denotes amount of energy that is absorbed by $\alpha\beta$ reflection of ij detector in n_{zL} copy of the xy-plane from the flash that occurs at (x_0, y_0, z_0), if there is no top face. Intensity of imaginary source is also considered.

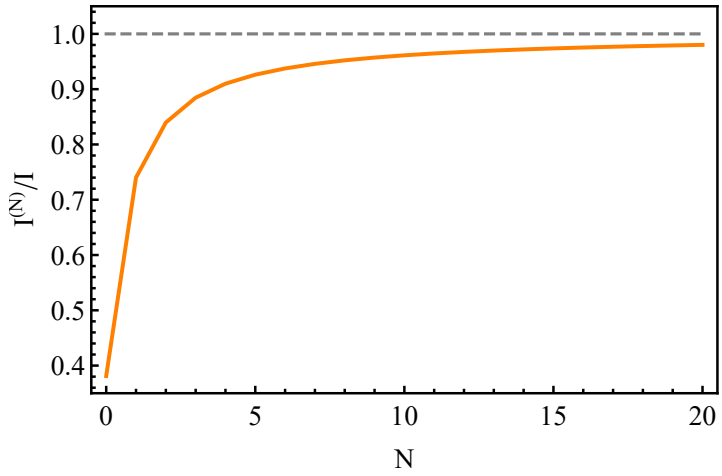

Figure 4: The dependence of $I^{(N)}/I$ on number of considered reflections N ($M = N$ is used). Flash occurs at $(5, -2, 3)$. Parameters are: $H = 7$, $n = 4$, $m = 3$, $a = 4$, $b = 5$. All reflection coefficients are equal to 1, except $p_{zL} = 0$.

3 Numerical implementation of Eq. (11) and Monte-Carlo simulation

3.1 Numerical implementation of Eq. (11)

An easy way to implement formula (11) numerically is to consider $\alpha \in \{-N, \dots, N\}$, $\beta \in \{-M, \dots, M\}$ and $n_{zL} \in \{0, \dots, K\}$. Numbers N, M and K should be chosen in the way that limits remaining terms in the sum at the needed level of error. Further, $I_{ij}^{(N)}$ denotes the intensity, achieved via this numerical approach. First, if $p_{zL} \ll 1$, numerical error can be evaluated next way:

$$\delta I = \left| I - I^{(N)} \right| \leq I \sum_{n_{zL}=0}^{+\infty} (1 - p_{zL}) p_{zL}^{n_{zL}} p_{zR}^{n_{zL}} \left(2\pi - \Delta\Omega_{n_{zL}}^{(x_0, y_0, z_0)} + p_{zR} \left(2\pi - \Delta\Omega_{n_{zL}}^{(x_0, y_0, 2H - z_0)} \right) \right) \simeq \tag{12}$$

$$\simeq I \left(2\pi - \Delta\Omega_0^{(x_0, y_0, z_0)} + p_{zR} \left(2\pi - \Delta\Omega_0^{(x_0, y_0, 2H - z_0))} \right) \right).$$

Here $\Delta\Omega_{n_{zL}}^{(x_0, y_0, z_0)}$ is spherical angle that is occupied by the rectangle that is formed out of considered reflections in n_{zL} plain from the point of view (x_0, y_0, z_0). The sizes of this rectangle are $(2N+1)L_x$, $(2M+1)L_y$. In Eq. (12) we neglected with terms that have $n_{zL} \neq 0$.

Let $r_m = \min((2N+1)L_x, (2M+1)L_y)$. If sizes of the mentioned rectangle are much larger than the height of scintillator (i.e. $(2N+1)L_x, (2M+1)L_y \gg H$), then in Eq. (12) $x_0 = 0$ and $y_0 = 0$ could be considered. Finally, the error can be evaluated as:

$$\frac{\delta I}{I} \simeq \frac{2\pi r_m z_0}{4\pi r_m^2} + p_{zR} \frac{2\pi r_m (2H - z_0)}{4\pi r_m^2} \simeq \frac{z_0}{2r_m} + p_{zR} \frac{2H - z_0}{2r_m} \sim \frac{1}{N} \tag{13}$$

In the Fig. 4 is depicted how total intensity on the detectors depends on number of considered reflections in Eq. (2). At $N = M = 20$ value $\delta I/I \simeq 0.03$.

However, if $p_{zL} \sim 1$, then a different number of reflections should be considered for different n_{zL} planes to retain the same spherical angle for errors.

3.2 Simple Monte-Carlo

To proof the concept of kaleidoscopic ray-traicing, we conducted a Monte-Carlo simulation of the uniform flash. In the Fig. 5 is depicted the dependence of $\delta I^{(N-MC)} = \sum_{i,j} |I_{ij}^{(N)} - I_{ij}^{(MC)}|/I$ on N – number of considered reflections in Eq. (11). Here $I_{ij}^{(MC)}$ denote intensity achieved on ij detector via Monte-Carlo simulation.

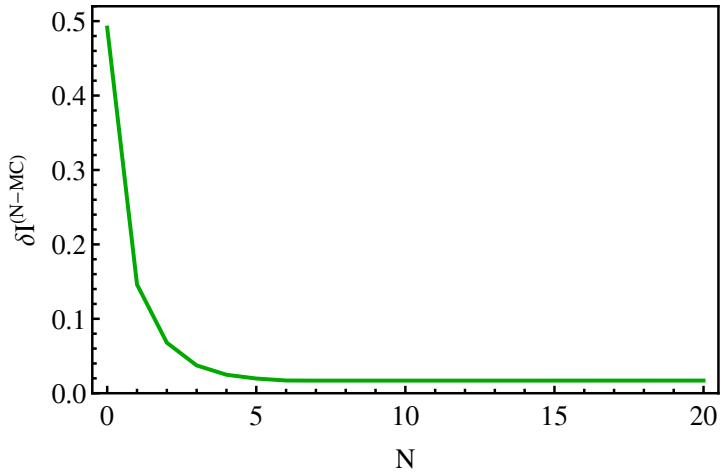

Figure 5: The dependence of $\delta I^{(N-MC)}$ on number of considered reflections N ($M = N$, $K = 10$ are used). Flash occurs at $(5, -2, 3)$. Parameters are: $H = 7$, $n = 4$, $m = 3$, $a = 4$, $b = 5$, $p_{xL} = 0.8$, $p_{xR} = 0.95$, $p_{yL} = 0.9$, $p_{yR} = 0.85$, $p_{zR} = 0.75$, $p_{zL} = 0.1$.

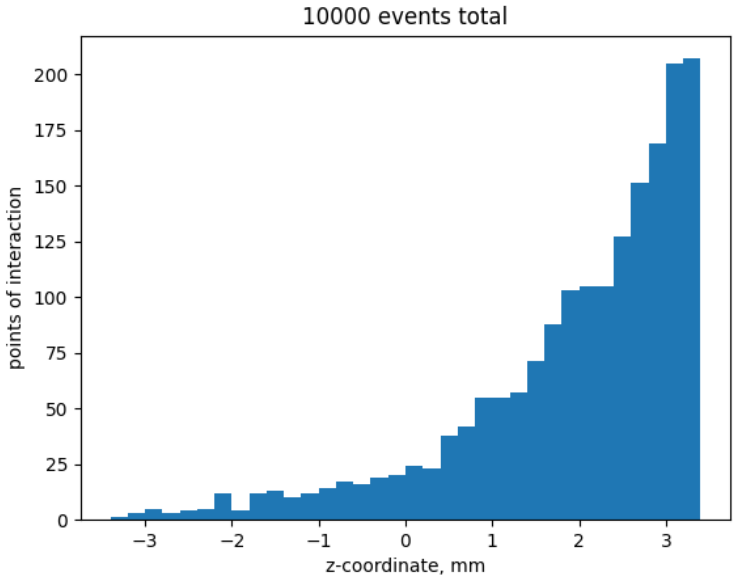

Figure 6: Simulated distribution of interaction points along the z-axis.

One can see that $\delta I^{(N-MC)}$ sharply decreases, while N is growing, and if $N > 20$, results achieved via Eq. (11) and Monte-Carlo simulation coincide. The vestigial error should be considered as the statistical error of the Monte-Carlo simulation.

3.3 Geant4

Geant4 [9] simulation toolkit is a widespread tool to simulate scintillation physics. Optical physics is represented by a separate module, implementing different models. In our case, it was a UNIFIED model, adopted from DETECT [10].

To test the Eq. (11) and compare it with GEANT4 results, GAGG: Ce [11] scintillator 14mm x 14mm x 7mm size was placed in the center. It means that the scintillator had a 3.5 mm maximum coordinate and a -3.5 mm minimum coordinate along the z-axis. Its lower face was covered with 4 equal squares of size 7 mm x 7 mm, that detected photons with a probability of 0.3, simulating SiPM's [12] (usually used as detectors) efficiency. The other faces were

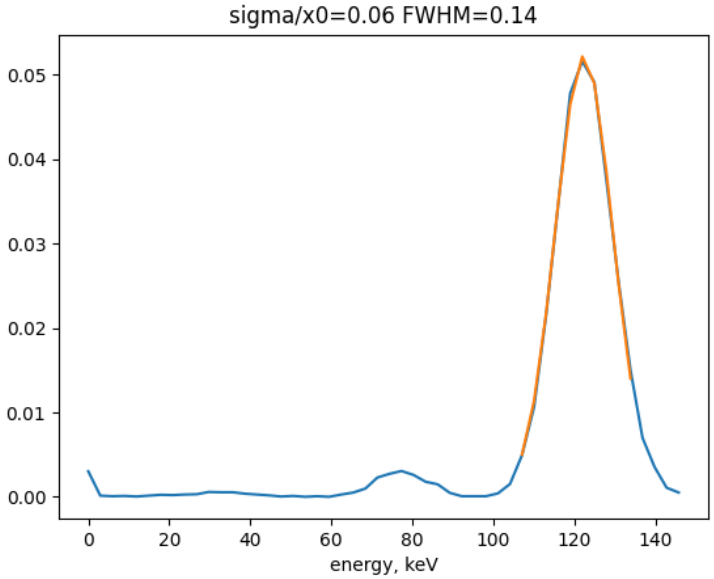

Figure 7: Simulated energy distribution.

covered with Tyvek [13] to simulate reflecting faces properties. There was also another setup with default UNIFIED dielectric-dielectric reflecting surfaces instead of Tyvek cover, and it showed the same average result. Then a 122 keV particle was launched into the scintillator along the z-axis.

There is one important factor that we should consider: there is no strict point of scintillation along the z-axis because particles penetrate the scintillator exponentially, as shown in Fig.6. The Eq. (11) was calculated with different z_0 coordinates, then averaged over the distribution. Here we make a rough guess that all interactions refer to the photo effect (leading to 100 percent energy loss), which is generally not true because there is a significant number of Compton scatterings too, as its shown in Fig. 7. The intensity I was calculated as scintillation yield of GAGG: Ce multiplied by 122 keV energy, then multiplied by 0.3 to consider SiPM's efficiency.

Predicted energy outcome on every detector and the GEANT4 results had 8 percent average relative difference. It means that the derived formula can be used in scintillation detectors with reflecting faces, a small number of detectors, and a relatively big distance between scintillation point and detectors, unlike Anger's method. The error can be reduced by removing all events below the peak in Fig. 7 and counting light yield distribution instead of simple events distribution along the z-axis. Scintillation flash in the simulated detector isn't a point, but it has some size, so it reduces precision too.

4 Anger method test

Eq. (2) can be used for testing the Anger method for localization of the flash. Anger method establishes coordinates of the flash next way [2–4]:

$$x_0^{(AM)} = \frac{\sum\limits_{ij} I_{ij} x_{ij}^{(c)}}{\sum\limits_{ij} I_{ij}}, \qquad y_0^{(AM)} = \frac{\sum\limits_{ij} I_{ij} y_{ij}^{(c)}}{\sum\limits_{ij} I_{ij}}, \tag{14}$$

with the cut-off for intensity.

From a general perspective, it's clear that this approach is reliable only if the amount of detector is large, wall faces and top face are fully absorbing, flash is placed nearly above the center of the bottom face (this reduces the amount of energy, that is absorbed by the wall faces and prevents "mass center" of the intensities from being shifted towards the center of the bottom face), and the flash happens at $z_0 \sim L_x, L_y$ to neglect with the non-linearity of Eq. (6).

To test the Anger method we placed the flash at $(1.75, 1, 5)$, and fixed $L_x = 16.0$, $L_y = 15.0$. The bottom face of the scintilator was split into $n \times n$ detectors. After that, we studied the dependence of the distance in xy plain between the

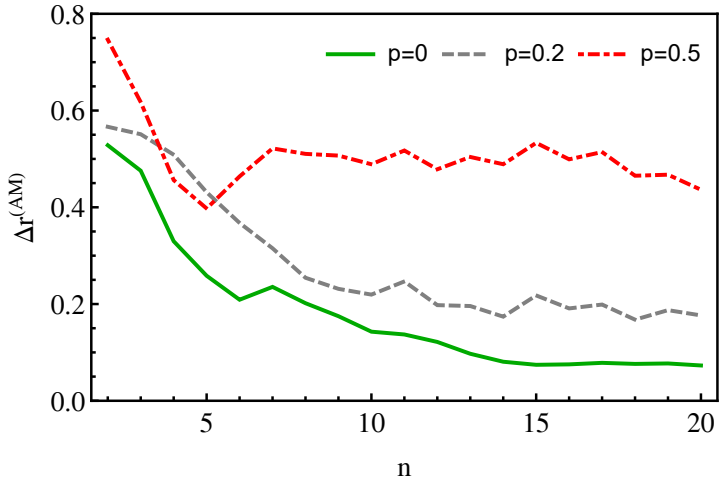

Figure 8: The dependence of moving average of $\Delta r^{(AM)}$ on n – square root out of number of detectors. Flash occurs at $(1.75, 1, 5)$. Parameters are: $H = 7$, $L_x = 16$, $L_y = 15$, $p_{zL} = 0$. Green (red, blue) line depicts the case when all reflective coefficients of walls are 0 (0.2, 0.5). Anger method is implemented with the half of the maximum cut-off for intensity.

flash and "the flash" localized via the Anger method on n:

$$\Delta r^{(AM)} = \sqrt{\left(x_0 - x_0^{(AM)}\right)^2 + \left(y_0 - y_0^{(AM)}\right)^2}. \tag{15}$$

The dependence of $\Delta r^{(AM)}$ on n is presented in Fig. 8. When all reflective indexes of walls are zero, the Anger method reconstructs x and y coordinates precisely. If reflective indexes of walls are nonzero, the Anger method involves sufficient errors that result in the shift of "the flash" comparable to the size of a detector. If flash happens more closely to one of the wall faces, the shift will be more sufficient.

However, if all reflective indexes are much less than 1, Anger's method still can be used as a starting point for iterative algorithms that minimize $\|\vec{F}(\vec{F}^{-1}(\vec{W})) - \vec{W}\|$.

5 Several important cases and restrictions of the method

5.1 Non-uniform flash

If the intensity of the flash has non-uniform distribution, Eq. (11) stays true. Formulas for degrees of reflective coefficients also stay true. However, Eqs. (3)-(6) should be modified. Let $P(\theta, \phi)$ be the angle distribution of intensity. One can use the next formula for intensity instead of Eq. (3):

$$I_A = \int\limits_A (\vec{S}, \vec{n}) P(\theta, \phi) dx dy = \int\limits_{x^{(L)}}^{x^{(L)}+a} dx \int\limits_{y^{(L)}}^{y^{(L)}+b} dy \frac{P(\theta, \phi)}{4\pi R^2} I \frac{z_0}{R}. \tag{16}$$

5.2 Technical scars on the detectors

In reality, detectors are separated one from another by borders with non-zero width due to the process of creation [4, 14]. Let the width of the line be 2κ. The non-zero width of borders reduces the amount of energy each of the detectors gets by reducing the spherical angle of the detector and it's reflections. The impact of this effect can be taken into account by inserting frames with width κ into all reflections of each detector. This way I_A should be calculated as:

$$I_A = \int\limits_{x^{(L)}+\kappa\chi_L}^{x^{(L)}+a-\kappa\chi_R} dx \int\limits_{y^{(L)}+\kappa\gamma_L}^{y^{(L)}+b-\kappa\gamma_R} dy \frac{I}{4\pi R^2} \frac{z_0}{R}. \tag{17}$$

Here $\chi_L = 1$, if $i > 1$; $\chi_R = 1$, if $i < n$; $\gamma_L = 1$, if $j > 1$; $\gamma_R = 1$, if $j < m$, otherwise these coefficients equal zero.

5.3 Restrictions of the method

To implement all the procedures that we stated above correctly, the shape of the mirror box should be one of the kaleidoscopic forms. This provides us with an important property of kaleidoscopes: if we reflect the space U into kaleidoscope over different walls several times finally getting the reflection U', the way how did U get to U' (over which wall it has been reflected and how many times) does not matter: the detector ij would be reflected into the same reflection [15].

This fact allows us to straighten reflected rays, being sure that rays that reach a reflection of the detector reach this detector in the bottom of the scintillator.

6 Conclusion

In this article, we developed an analytical approach (kaleidoscopic ray-tracing) to intensity calculation in scintillation detectors with semi-reflecting faces and a matrix of photodetectors. The developed approach is based on kaleidoscopic reflection of detecting face over reflecting faces. This trick results in a calculation of several infinite sums that converge fast. Numerical implementation of the developed approach involves errors that also are estimated analytically.

We conducted two Monte-Carlo simulations to check the results achieved via an analytical approach. The first one involved only geometrical optics principles, and the second one has been made by means of Geant4 [9] simulation toolkit, which also involves nuclear physics of the scintillation process, non-point source of light, fluctuations in the number of photons, and so on. Both of them are in good agreement with the developed analytical approach. This method may be more convenient for real-time calculations than the usage of pre-calculated Monte Carlo tables of coordinate versus intensity due to the ability to calibrate some parameters without running a new Monte Carlo simulation.

Also, we tested the Anger method of flash localization using the results achieved via the developed analytical approach. It showed that even under quite favorable conditions, the Anger method shifts the flash on the distance, which is comparable with the size of the individual detector. Under non-favorable conditions, the Anger method may result in sufficient errors.

Developed analytical method of intensity calculation in multi-mirror systems discover new possibilities for localization of the flash in the scintillation detectors. Careful investigation of this statement we leave on further research.

References

[1] A. J. González, S. Majewski, J. Proffitt, A. Aguilar, P. Conde, L. Hernandez, F. Sánchez, A. Stolin, and J. M. Benlloch, "Continuous or pixelated scintillators?, not longer a discussion," in *2014 IEEE Nuclear Science Symposium and Medical Imaging Conference (NSS/MIC)*, 2014, pp. 1–4.

[2] H. O. Anger, "Sensitivity, resolution, and linearity of the scintillation camera," *IEEE Transactions on nuclear science*, vol. 13, no. 3, pp. 380–392, 1966.

[3] T. D. Milster, L. Selberg, H. H. Barrett, R. Easton, G. Rossi, J. Arendt, and R. Simpson, "A modular scintillation camera for use in nuclear medicine," *IEEE transactions on nuclear science*, vol. 31, no. 1, pp. 578–580, 1984.

[4] C. Fiorini, P. Busca, R. Peloso, A. Abba, A. Geraci, C. Bianchi, G. Poli, G. Virotta, K. Erlandsson, B. Hutton, *et al.*, "The HICAM gamma camera," *IEEE Transactions on Nuclear Science*, vol. 59, no. 3, pp. 537–544, 2012.

[5] M. Kim, B. H. Hong, I. Cho, C. Park, S.-H. Min, W. T. Hwang, W. Lee, and K. M. Kim, "Design of a scintillator-based prompt gamma camera for boron-neutron capture therapy: Comparison of sri2 and gagg using monte-carlo simulation," *Nuclear Engineering and Technology*, vol. 53, no. 2, pp. 626–636, 2021.

[6] A. Morozov, V. Solovov, F. Alves, V. Domingos, R. Martins, F. Neves, and V. Chepel, "Iterative reconstruction of detector response of an anger gamma camera," *Physics in Medicine & Biology*, vol. 60, no. 10, p. 4169, 2015.

[7] L. Landau and E. Lifchitz, "Theoretical physics. field theory," in Pergamon Press, 2004, pp. 170–177.

[8] J. H. Poynting, "On the transfer of energy in the electromagnetic field," *Philosophical Transactions of the Royal Society of London*, vol. 175, pp. 343–361, 1884.

[9] S. Agostinelli and et al., "Geant4—a simulation toolkit," *Nuclear instruments and methods in physics research section A: Accelerators, Spectrometers, Detectors and Associated Equipment*, vol. 506, no. 3, pp. 250–303, 2003.

[10] A. Levin and C. Moisan, "A more physical approach to model the surface treatment of scintillation counters and its implementation into DETECT," in *1996 IEEE Nuclear Science Symposium. Conference Record*, IEEE, vol. 2, 1996, pp. 702–706.

[11] Y. Zhu, S. Qian, Z. Wang, H. Guo, L. Ma, Z. Wang, and Q. Wu, "Scintillation properties of GAGG:Ce ceramic and single crystal," *Optical Materials*, vol. 105, p. 109 964, 2020.

[12] F. Acerbi and S. Gundacker, "Understanding and simulating SiPMs," *Nuclear Instruments and Methods in Physics Research Section A: Accelerators, Spectrometers, Detectors and Associated Equipment*, vol. 926, pp. 16–35, 2019.

[13] L. Nozka, M. Pech, H. Hiklova, D. Mandat, M. Hrabovsky, P. Schovanek, and M. Palatka, "BRDF profile of tyvek and its implementation in the geant4 simulation toolkit," *Optics Express*, vol. 19, no. 5, pp. 4199–4209, 2011.

[14] D. R. Schaart, H. T. van Dam, S. Seifert, R. Vinke, P. Dendooven, H. Löhner, and F. J. Beekman, "A novel, sipm-array-based, monolithic scintillator detector for pet," *Physics in Medicine & Biology*, vol. 54, no. 11, p. 3501, 2009.

[15] K.-D. Graf and B. R. Hodgson, "Popularizing geometrical concepts: The case of the kaleidoscope," *For the Learning of Mathematics*, vol. 10, no. 3, pp. 42–50, 1990.